Res Mechanica **25** (1988) 171–181

Influence of Uncertainties About Depth and Epicentral Location of Earthquakes on Seismic Hazard Analysis

M. Chávez

Instituto de Ingenieria, UNAM, Apdo. 70–569, 04510 México, DF, México

(Received 30 November 1987)

ABSTRACT

A methodology is proposed to incorporate the uncertainties about epicentral location and depth of earthquakes on seismic hazard analysis. The procedure utilizes Monte-Carlo simulation and Bayesian statistics techniques. Parametric studies and a real case problem are included. The results of these studies have shown that the effects of the uncertainties about the location of earthquakes on the seismic hazard estimated for a site are (at least) as important as the associated uncertainties related to the attenuation relations.

1 INTRODUCTION

It is a common practice in seismic hazard studies for a site or region to use raw data regarding the location parameters of seismic events from world catalogs of events: this data is used as input to seismic hazard models from which the seismic hazard at a site is estimated. Recent studies have shown that there is a systematic mislocation of shallow events in subduction zones from teleseismic data. As the location parameters play an important role in the determination of the ground motion intensities at a site—through the attenuation relations used in the study—its mislocation has an effect on the estimated hazard for a site.

A procedure is proposed in this paper to incorporate the uncertainties about epicentral location E and depth H of earthquakes on

Res Mechanica 0143-0084/88/$03·50

seismic hazard analysis. The procedure makes use of Bayesian statistics, Monte-Carlo simulation and point estimate techniques, to include the uncertainties into the seismic hazard model. Parametric studies and a real case problem are included. From these studies the influence of the uncertainties about the location parameters of earthquakes on the seismic hazard estimated for a site is highlighted.

2 DATA

In a recent paper, Singh and Lermo[1] compared the locations of several Mexican large shallow events and their aftershocks, determined from field seismographs or from particular studies (to be referred to as local events) with those reported in the Preliminary Determination of Epicenters (PDE) and in the International Seismological Centre (ISC) bulletins. They concluded that in general both bulletins reported epicenters shifted tens of kilometers from their actual locations; also the depths given in those bulletins showed a disagreement of that order with respect to the locally determined events. Those authors suggested that the mislocations are probably due to the higher velocity of the Cocos plate below Mexico. These types of mislocations have also been reported for other subduction zones, for example in Japan,[2] Tonga[3] and the Aleutians.[4]

Table 1 shows the epicentral locations and depths of the 33 out of 35 events used by Singh and Lermo.[1] Also their surface magnitudes (M_s) are included in the table; some of those magnitudes were converted from the body wave magnitudes reported by those authors. The information about the locally determined events (Local in Table 1) was taken as the actual one for the events and it was assumed (after Ref. 1) that the corresponding values in the PDE and ISC bulletins had errors in E and H. It was also assumed that there were no errors in the magnitudes included in Table 1. The error in the epicentral locations (e) and in the depths (h) were computed as the absolute values of the differences between the values reported by the Local and the PDE, and the former and the ISC catalogs. From the values of e and h for the PDE and ISC catalogs, their mean ($\bar{e}$, $\bar{h}$) and standard deviation (σe, σh) values were computed and provided the following results: for PDE, $\bar{e} = 37{\cdot}01$ km, $\sigma e = 18{\cdot}53$ km, $\bar{h} = 17{\cdot}85$ km, $\sigma h = 10{\cdot}77$ km and for ISC, $\bar{e} = 46{\cdot}59$ km, $\sigma e = 31{\cdot}65$ km, $\bar{h} = 26{\cdot}69$ km, $\sigma h = 24{\cdot}28$ km. In Figs 1 to 4 the histograms computed for the e and h of each catalog are shown. In order to find which probability distribution best fitted those histograms, several tests were performed and the lognormal distributions provided that

TABLE 1
Epicentral Locations, Depths and Surface Magnitudes (M_s) of the 33 Events used in this Study (after Ref. 1).

	Local			*PDE*			*ISC*			
Date	*Lat N* (°)	*Long W* (°)	*Depth* (km)	*Lat N* (°)	*Long W* (°)	*Depth* (km)	*Lat N* (°)	*Long W* (°)	*Depth* (km)	M_s
30 Jan. 73	18·39	103·21	32·0	18·48	103·00	43·0	18·53	102·93	48·0	7·5
10 Feb. 73	18·41	103·63	11·0	18·89	103·55	33·0	18·78	103·79	42·0	5·6
29 Nov. 78	16·00	96·69	18·0	16·01	96·59	18·0	16·07	96·55	23·0	7·7
2 Dec. 78	15·53	96·68	13·0	15·79	96·48	50·0	15·81	96·47	36·0	4·6
2 Dec. 78	15·57	96·73	12·0	15·85	96·49	33·0	16·08	96·39	21·0	4·0
2 Dec. 78	15·48	96·73	10·0	15·75	96·52	33·0	15·83	96·48	23·0	4·8
2 Dec. 78	15·73	96·82	13·0	16·02	96·44	33·0	16·07	96·39	50·0	4·4
5 Dec. 78	15·72	97·30	11·0	16·06	96·98	33·0	16·10	96·93	31·0	4·3
5 Dec. 78	15·60	96·75	24·0	15·95	96·58	33·0	15·91	96·54	34·0	4·7
8 Dec. 78	15·80	96·78	19·0	15·67	96·52	33·0	15·70	96·49	53·0	3·2
11 Dec. 78	15·50	96·85	15·0	15·75	96·62	33·0	15·70	96·69	19·0	3·2
14 Mar. 79	17·46	101·46	20·0	17·81	101·28	49·0	17·76	101·30	3·0	7·6
14 Mar. 79	17·40	101·40	16·0	17·71	101·08	61·0	17·80	100·90	104·0	4·2
16 Mar. 79	17·34	101·38	25·0	17·99	101·15	33·0	18·00	100·70	106·0	4·2
18 Mar. 79	17·42	101·10	25·0	17·55	100·99	33·0	17·72	100·89	61·0	5·4
20 Mar. 79	17·34	101·44	30·0	17·53	101·29	51·0	17·57	101·26	56·0	4·8
22 Mar. 79	17·74	101·65	30·0	17·96	101·54	76·0	18·02	101·52	77·0	5·0
28 Mar. 79	17·41	101·16	30·0	17·14	101·04	42·0	17·20	100·60	99·0	4·3
6 Apr. 79	17·45	101·63	14·0	16·76	102·12	51·0	17·40	101·50	100·0	4·6
25 Oct. 81	17·75	102·25	16·0	18·05	102·08	33·0	18·18	102·01	28·0	7·3
28 Oct. 81	17·89	102·35	15·0	18·46	102·48	33·0	16·30	102·90	33·0	3·6
7 Jun. 82	16·38	98·38	20·0	16·61	98·15	41·0	16·51	98·25	19·0	6·9
7 Jun. 82	16·48	98·55	15·0	16·56	98·36	34·0	16·58	98·34	20·0	7·0
8 Jun. 82	16·40	98·39	38·0	16·37	98·36	33·0	15·90	98·41	61·0	3·9
9 Jun. 82	16·59	98·44	23·0	16·66	98·33	33·0	16·86	98·38	52·0	4·8
9 Jun. 82	16·36	98·51	15·0	16·57	98·28	33·0	16·54	98·22	53·0	4·4
13 Jun. 82	16·16	98·44	20·0	16·18	98·40	33·0	16·00	98·50	33·0	3·9
13 Jun. 82	16·51	98·40	25·0	16·26	98·44	6·0	16·28	98·42	7·0	3·9
13 Jun. 82	16·50	98·40	25·0	16·13	98·39	33·0	16·10	98·42	33·0	3·4
13 Jun. 82	16·56	98·44	27·0	16·18	98·37	34·0	16·30	98·29	41·0	3·6
14 Jun. 82	16·36	98·30	26·0	16·60	98·05	40·0	16·55	98·05	46·0	4·7
15 Jun. 82	16·55	98·27	24·0	16·30	98·10	33·0	15·90	98·00	33·0	3·8
15 Jun. 82	16·63	98·47	30·0	16·46	98·38	38·0	16·65	98·36	38·0	3·6

fitting. The resulting distributions are presented in Figs 1 to 4. Further results are given elsewhere.[5]

3 PROCEDURE

Once a located site and region are known, and a catalog has been selected, the following procedure can be applied to incorporate the

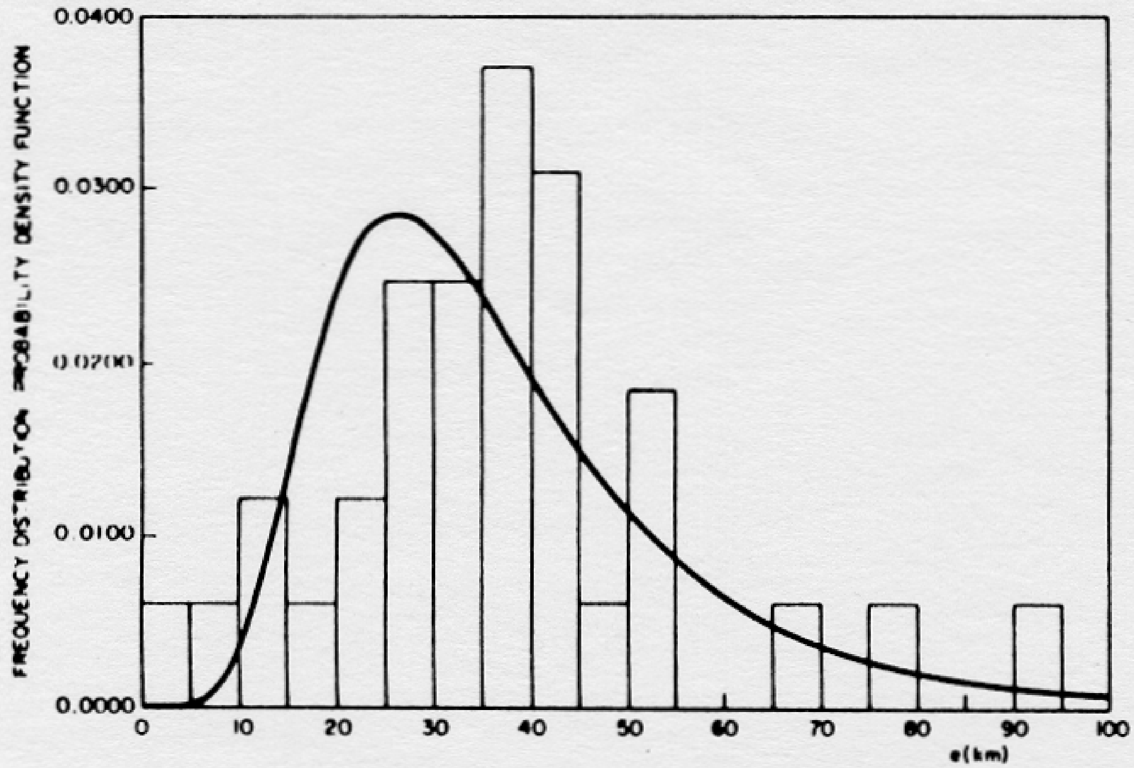

Fig. 1. Histogram of the error in the epicentral location e for the PDE catalog and its fitted lognormal distribution with median $\bar{m}_e = 33{\cdot}09$ km and standard deviation of the natural logarithm $\sigma_{\ln e} = 0{\cdot}4731$.

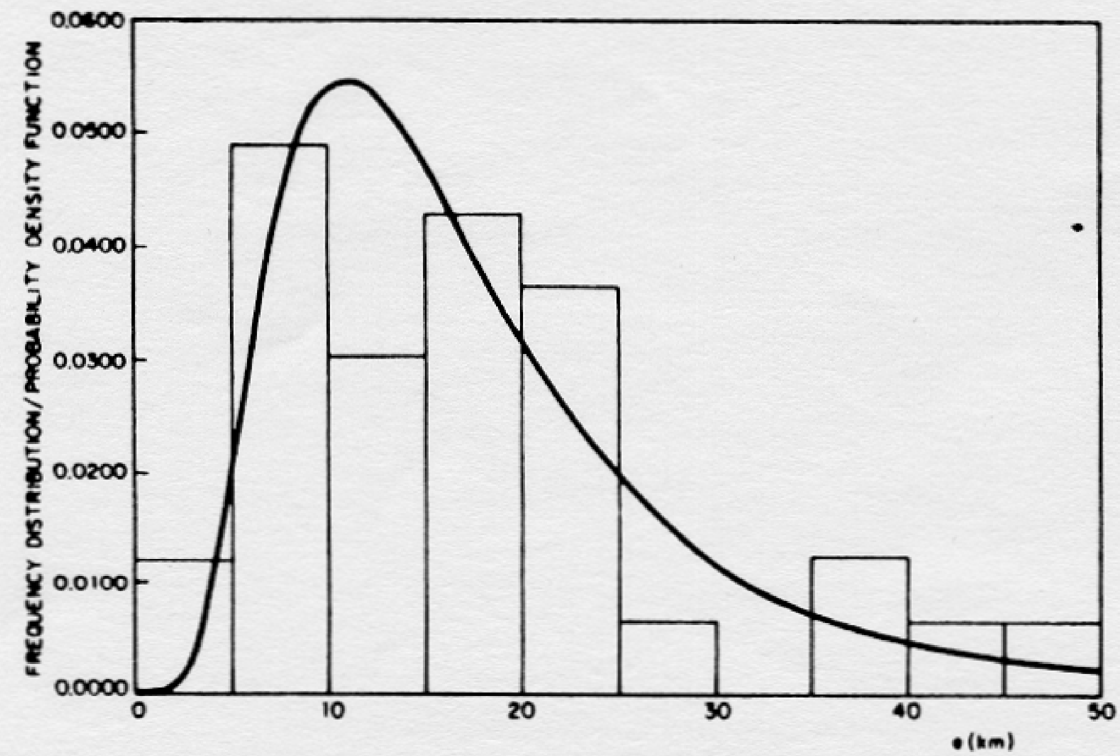

Fig. 2. Histogram of the error in the depth h for the PDE catalog and its fitted lognormal distribution with median $\bar{m}_z = 15{\cdot}28$ km and standard deviation of the natural logarithm $\sigma_{\ln z} = 0{\cdot}5573$.

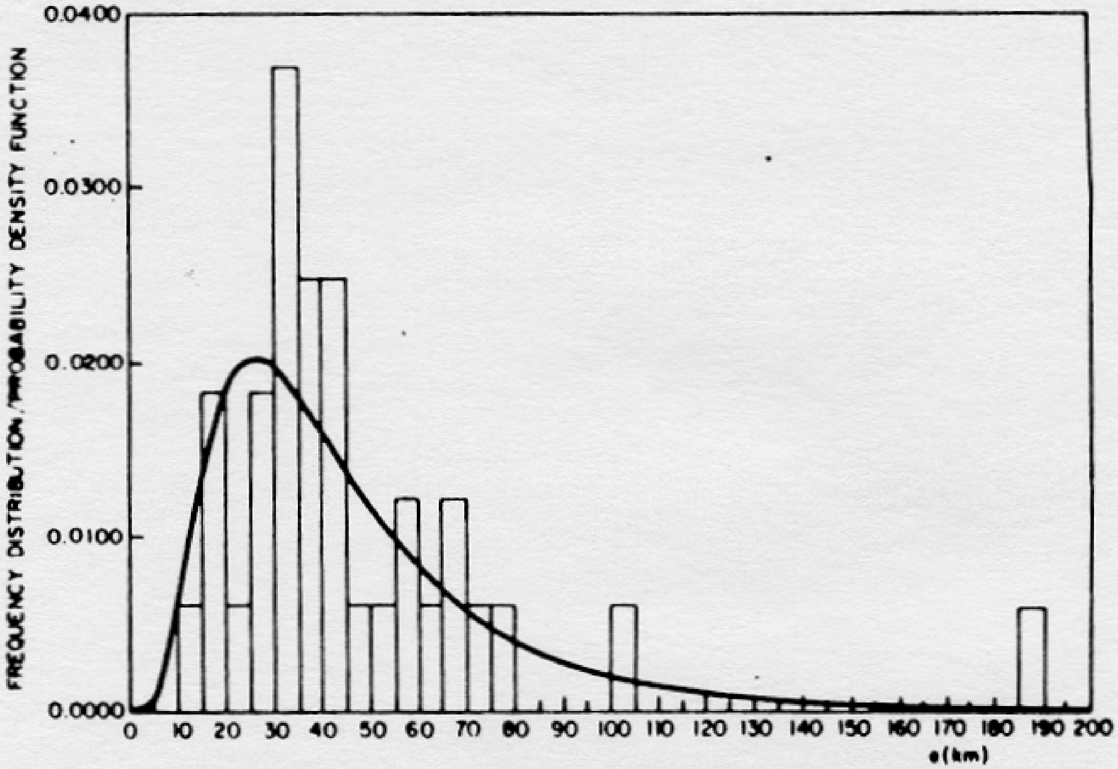

Fig. 3. Histogram of the error in the epicentral location *e* for the ISC catalog and its fitted lognormal distribution with median $\hat{m}_e$ = 38·54 km and standard deviation of the natural logarithm $\sigma_{\ln e}$ = 0·6160.

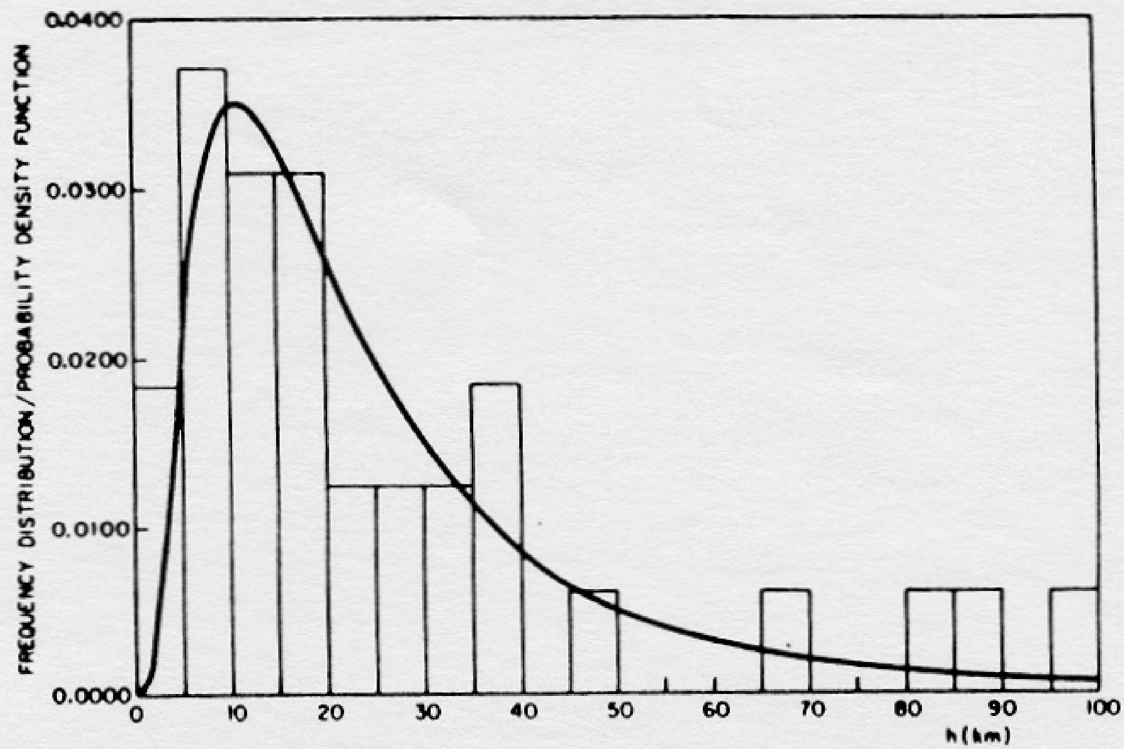

Fig. 4. Histogram of the error in the depth *h* for the ISC catalog and its fitted lognormal distribution with median $\hat{m}_h$ = 19·88 km and standard deviation of the natural logarithm $\sigma_{\ln h}$ = 0·7675.

effect of uncertainties about E and H in the seismic hazard analysis: 1) determine the probability distribution of the error in E and H implicit in the catalog;[5] 2) obtain a random sample of e and h values for each of the events of the catalog from their respective distribution, sample size $N > 100$; 3) generate a sample of epicentral distance, E', and depth, H', for each of the events of the catalog by randomly adding or subtracting to their respective E and H, the e and h generated in 2); 4) obtain the ground motion intensities associated to the E', H' and M, of the sample of each event, by using an appropriate attenuation relation; 5) compute the excedance rates for each of the events of the catalog; 6) calculate for each of the excedance rates the probability of excedance of their associated ground intensities by following Gumbel's criteria. This implies that the accumulated probability distributions of the ground intensities are of the extreme type, and also that each of those intensities correspond to independent events; 7) select for each of the excedance rates the ground intensities with the same value of the probability of excedance of interest; 8) compute, for the data obtained in 7) the rate of occurrence $v(y)$ with the expression

$$v(y) = ay^{-b}\,(1 - (y/y_1)^c) \tag{1}$$

where y is the ground motion intensity of interest, a, b, c, depend on the seismicity of the region where the site is located and y_1 is the maximum y which may occur at the site. The estimation of these parameters can be achieved by using bayesian statistics and point estimate techniques, and therefore one is able to actualize the $v(y)$ when new data is available;[6] 9) compute the expected $v(y)$ when the uncertainties about the attenuation relation used are taken into account.[6]

4 PARAMETRIC STUDY

A parametric study was performed with the procedure proposed in Section 3. The objectives of the study were the following: a) to compare the effect on the seismic hazard for a site of the uncertainties on E and H implicit in the PDE and ISC catalogs, with respect to the seismic hazard calculated for the local catalog (Table 1); b) to compare the same effect with respect to the effect of the uncertainties related to the attenuation relation used in the study.

The chosen site has coordinates 17·5 °N, 98·75 °W and is located in the region enclosed by the latitudes 15 ° to 19 °N and longitudes 96 ° to 104 °W, this site is identified as S_1 in Fig. 5. All the events of Table 1 occurred in this region. In Fig. 5 the epicenters of the main events

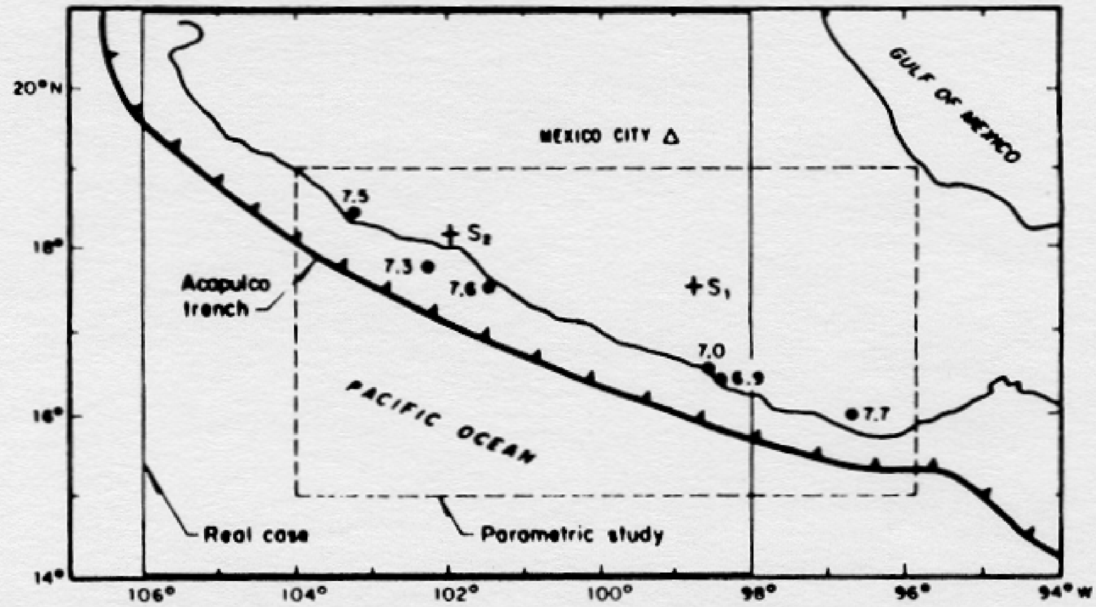

Fig. 5. Location of the sites for the parametric study and for the real case. Also, the epicenters of the main shocks included in Table 1 are shown.

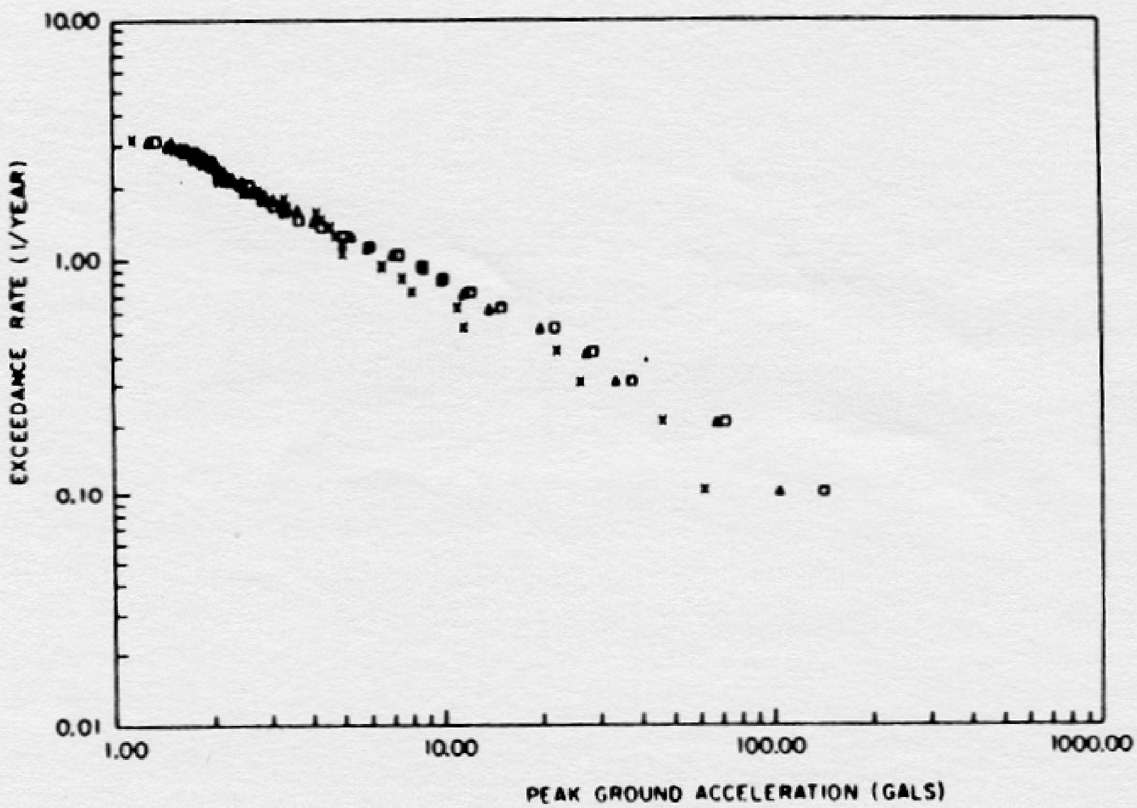

Fig. 6. Rate of excedance of peak ground accelerations for the local (X), PDE_{10} (Δ) and ISC_{10} (□) data, the later are for the 10% probability of excedance of the ground intensities.

(according to the local catalog) are shown. The y of interest is the peak ground acceleration, computed by the relation proposed by Esteva and Villaverde[7]

$$y = 5600 \exp(0{\cdot}8\,M)\,(R + 40)^{-2} \qquad (\mathrm{cm/s^2}) \qquad (2)$$

where $R = \sqrt{E^2 + H^2}$, $M = M_r$. A y_1 value of 300 Gal (1 gal = 1 cm/s²) was assumed and $N = 1000$ was used in the simulation step 2. The correction of $v(y)$ associated with the uncertainties on the expression (2) was performed as proposed by Esteva and Chavez.[6]

The results of the study are shown in Figs 6 to 8. In Fig. 6 the data for the local catalog and those corresponding to the PDE and ISC data are shown. The subindex 10 means that there is a 10% probability of excedance of the peak ground accelerations associated with a particular v (step 5 of the procedure). In Fig. 7 the $v(y)$ resulting from applying step 8 to the data sets of Fig. 6 are shown. From this figure it can be concluded that for a given v the peak ground acceleration y is larger for the PDE and ISC data sets. This effect is stressed for certain ranges of y and is larger for the ISC data. Finally, in Fig. 8 it is shown that the effect of the uncertainties in E and H, of the ISC catalog, on the

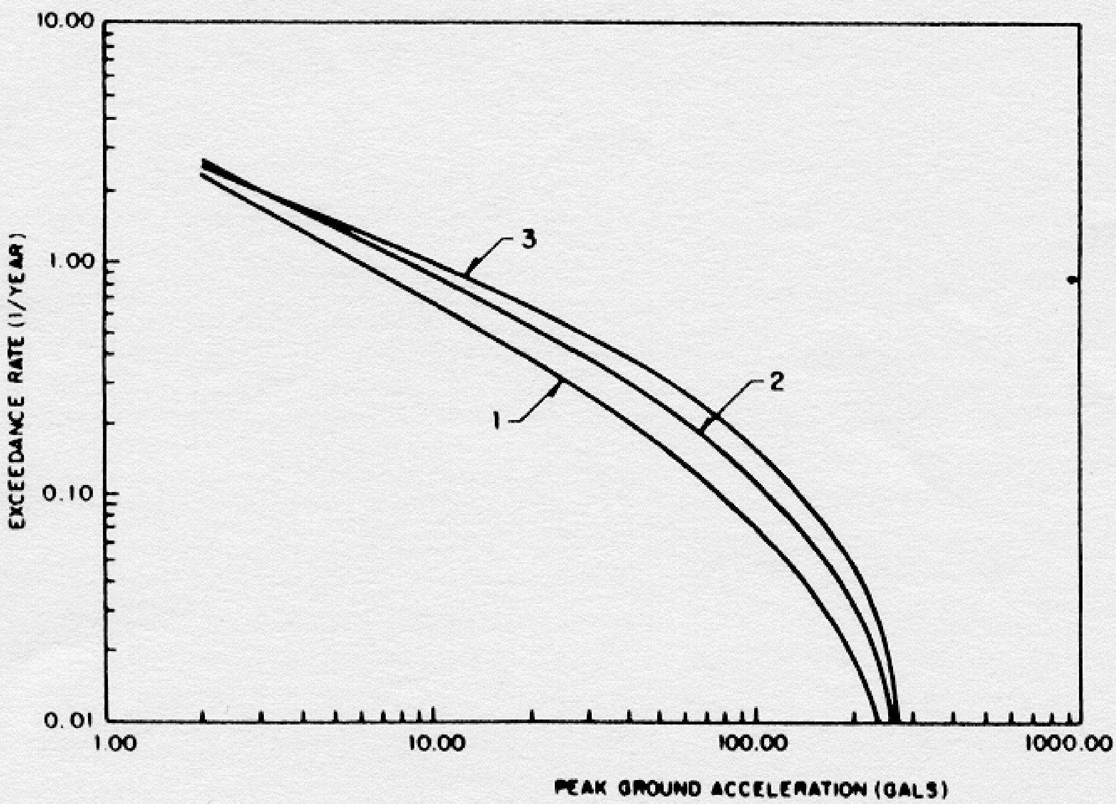

Fig. 7. $v(y)$ computed for each of the data sets shown in Fig. 6. Local (1); PDE_{10} (2); ISC_{10} (3). (See Fig. 6 for symbology.)

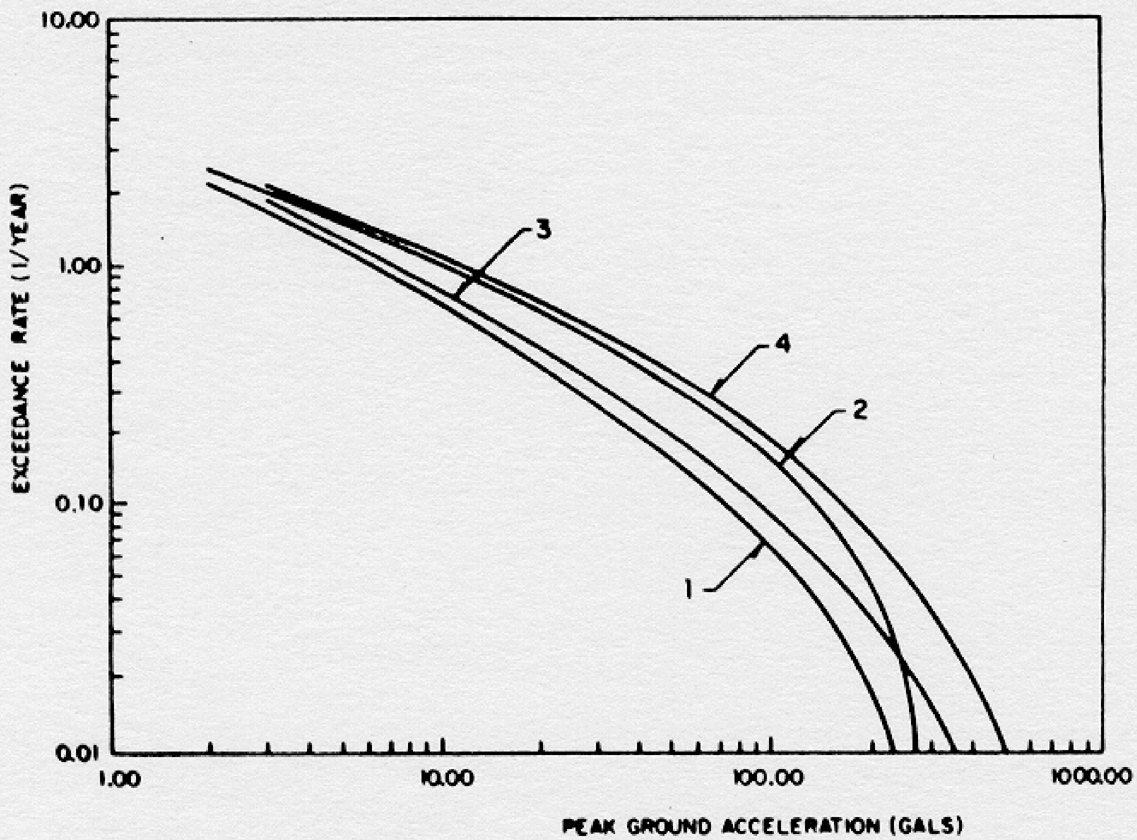

Fig. 8. $v(y)$ computed for the original ISC catalog (1); for the ISC_{10} (2) and their corresponding $v_r(y)$ corrected by uncertainties on the attenuation relation used; original ISC (3); ISC_{10} (4). (See Fig. 6 for symbology.)

seismic hazard at the site are of the same order, as those related to the uncertainties on the attenuation relation used in the study.

5 APPLICATION TO A REAL CASE

The proposed procedure was applied to a site with coordinates 18·2 °N, 102 °W, located in a region defined by the latitudes 14 ° to 21 °N and longitudes 98 ° to 106 °W. The site is shown as S_2 in Fig. 5. Notice that about 50% of the area of this region coincides with the one used in the parametrical study. The catalog used was from the ISC. Equation (2) was utilized to calculate the y values. $N = 1000$ for the simulation of E' and H'. By using the seismotectonic information available for the region a y_1 value of 700 (gals) was used. The results of the application are shown in Fig. 9. From this figure it can be concluded that the effect of the uncertainties about E and H on the seismic hazard estimated for the site are as important as that related to the attenuation relation.

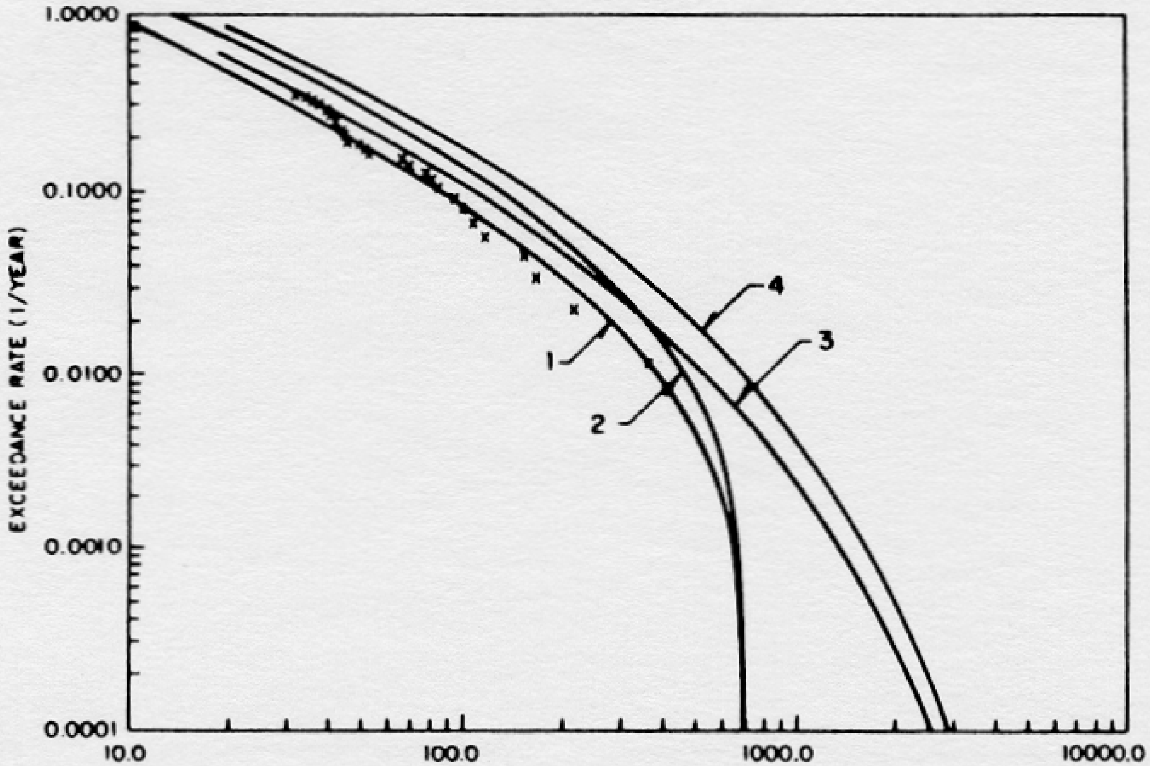

Fig. 9. $v(y)$ computed for a real case: data (X); original ISC catalog (1); ISC_{10} (2), and their corresponding $v_r(y)$ corrected by uncertainties on the attenuation relation used; original ISC (3); ISC_{10} (4).

6 CONCLUSIONS

1) The effects of the uncertainties about E and H on the seismic hazard estimated for a site are (at least) as important as the associated uncertainties related to the attenuation relation. 2) This effect can be incorporated in the hazard analysis by using a methodology as the one proposed in this paper. 3) Efforts should be dedicated to the determination of probability distributions of the errors on E and H for the seismic region of interest.

REFERENCES

1. Singh, S. K. & Lermo, J., Mislocation of Mexican earthquakes as reported in international bulletin. *Geofisica Internacional*, **24**(2) (1986) 333–52.
2. Utsu, T., Seismological evidence for anomalous structure of island arcs with special reference to the Japanese region. *Rev. Geophys. Space Phys.*, **9** (1971) 839–90.
3. Mitronovas, W., Isacks, B. & Seeber, L., Earthquake locations and seismic wave propagation in the upper 250 km of the Tonga island arc. *Bull. Seism Soc. Am.*, **59** (1969) 1115–35.

4. Engdahl, E. R., Dewey, J. W. & Fujita, K., Earthquake locations in island arcs. *Phys. Earth Planet. Interiors*, **30** (1982) 145–56.
5. Chavez, M., Vega, R., Jimenez, G. & Monroy, R., Uncertainties about epicentral distance and depths of Mexican subduction earthquakes and their influence on the evaluation of seismic risk at a site. Report No DE-15 Instituto de Ingenieria, UNAM Mexico DF, Mexico (1988).
6. Esteva, L. & Chavez, M., Analysis of uncertainty on seismic risk estimates. *Proc. 3rd Int. Earthquake Microzonation Conf. III*, 1982, pp. 1273–83.
7. Esteva, L. & Villaverde, R., Seismic risk, design spectra and structural reliability. *Proc. 5th WCEE Rome II*, 1973, pp. 2586–97.